Journal of Environmental Radioactivity 261 (2023) 107138

Contents lists available at ScienceDirect

Journal of Environmental Radioactivity

journal homepage: www.elsevier.com/locate/jenvrad

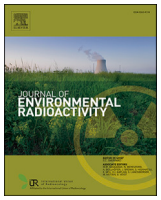

Some considerations on the dependence to numerical schemes of Lagrangian radionuclide transport models for the aquatic environment

R. Periáñez [a,*], I. Brovchenko [b], K.T. Jung [c], K.O. Kim [d], L. Liptak [e], A. Little [f], T. Kobayashi [g], V. Maderich [b], B.I. Min [h], K.S. Suh [h]

[a] Dpt Física Aplicada I, ETSIA Universidad de Sevilla, Ctra Utrera km 1, 41013-Sevilla, Spain
[b] Institute of Mathematical Machine and System Problems, Glushkov av., 42, Kiev 03187, Ukraine
[c] Environmental Research Institute of Oceanic Co. Ltd., 403 Munlnva-Building, 90 Yangpyung-ro, Yeongdeungpo-gu, Seoul, Republic of Korea
[d] Korea Institute of Ocean Science and Technology, 385, Haeyang-ro, Yeongdo-gu, Busan Metropolitan City, Republic of Korea
[e] AB Merit s.r.o., Hornopotocna 1, 917 01 Trnava, Slovakia
[f] Defence Academy of the United Kingdom, HMS Sultan, Military Road Gosport, Hampshire P012 3BY, UK
[g] Japan Atomic Energy Agency, 2-4 Shirakata Shirane, Tokai, Ibaraki 319-1195, Japan
[h] Korea Atomic Energy Research Institute, Daedeok-Daero 989-111, Yuseong-Gu, Daejeon, Republic of Korea

ARTICLE INFO

Keywords:
Radionuclides
Transport
Aquatic environment
Lagrangian model

ABSTRACT

Lagrangian models present several advantages over Eulerian models to simulate the transport of radionuclides in the aquatic environment in emergency situations. A radionuclide release is simulated as a number of particles whose trajectories are calculated along time and thus these models do not require a spatial discretization (although it is always required in time). In this paper we investigate the dependence of a Lagrangian model output with the grid spacing which is used to calculate concentrations from the final distribution of particles, with the number of particles in the simulation and with the interpolation schemes which are required because of the discrete nature of the water circulation data used to feed the model. Also, a Lagrangian model may describe the exchanges of radionuclides between phases (liquid and solid), which is done in terms of transition probabilities. The dependence of these probabilities with time step is analyzed as well. It was found that the optimum grid size used to calculate concentrations should be carefully checked, and that temporal interpolation is more significant than spatial interpolation to obtain a more accurate solution. A method to estimate the number of particles required to have a certain accuracy level is proposed. Finally, it was found that for low sediment concentrations and small radionuclide k_d, exact equations for the transition probabilities should be used; and that phase transitions introduce a stability condition as in Eulerian models.

1. Introduction

Generally speaking, two types of transport models are applied for simulating the transport of radionuclides in the aquatic environment: Eulerian and Lagrangian models (Periáñez et al., 2019a). Eulerian models are based on the solution of a differential equation to obtain the temporal evolution of the radionuclide concentration in water over the domain of interest. A radionuclide release is simulated by a number of particles in a Lagrangian model. The trajectory followed by each particle is calculated along the simulation time and, finally, the concentration of radionuclides is obtained from the number of particles per water volume unit. Many examples of Lagrangian models applied to radionuclide transport are found in literature (Schonfeld, 1995; Harms et al., 2000; Periáñez and Elliott, 2002; Periáñez, 2005a; Nakano et al., 2010; Kawamura et al., 2011; Kobayashi et al., 2007; Min et al., 2013; Periáñez et al., 2016, among many others).

Lagrangian models are specially well suited to asses radionuclide concentrations after an accidental release, since they do not introduce numerical diffusion and thus can handle the very high concentration gradients between contaminated and clean water which would be expected after an acute radionuclide release into the sea. Actually, numerical diffusion is one of the disadvantages of Eulerian models. It consists of (see for instance Kowalik and Murty, 1993) an artificial smoothing of concentration gradients produced by the numerical scheme used to

* Corresponding author.
E-mail address: rperianez@us.es (R. Periáñez).

https://doi.org/10.1016/j.jenvrad.2023.107138
Received 4 May 2020; Received in revised form 10 February 2023; Accepted 11 February 2023
Available online 24 February 2023

solve the advection terms in the differential equation describing the time evolution of radionuclide concentrations in an Eulerian model.

In addition, Lagrangian computations can be significantly faster than in Eulerian models when the contaminated area initially is a small part of the whole computational domain and if the number of particles in the simulation can be not too large (typically a few tens of thousands). This is an advantage in emergency modelling, when a fast response must be forwarded to decision–makers. Also, a real point source may be defined in Lagrangian models: the initial patch size is defined by the grid spatial resolution in Eulerian models. Consequently, lower peak concentrations are expected if Eulerian models are used.

Finally, the numerical solution of a differential equation required in Eulerian models implies the verification of several stability conditions to guarantee a stable solution (Kowalik and Murty, 1993). This limits the maximum time step which can be used in an Eulerian model and, thus, can significantly increase the computational time. Moreover, Lagrangian algorithms are easily parallelized, making it possible to calculate with $\sim 10^7$ particles (Suh et al., 2021).

However, water circulation must be known of course in both Eulerian and Lagrangian models to evaluate advection and diffusion. Water currents are obtained from an ocean circulation model and consequently consist of discrete data. Currents are specified at the nodes of the computational grid used in the hydrodynamic model and at discrete time intervals. Thus, interpolation schemes in time and space must be used by the Lagrangian model in order to evaluate the water velocity at the exact particle position and at the desired moment. Also, a grid is required in the Lagrangian model to calculate the radionuclide concentration from the number of particles per water volume unit. Usually, for computational economy, this grid is the same used to define water currents (the same grid used in the hydrodynamic model), but can be defined arbitrarily. It should be noted, however, that methods which do not use a grid (e.g. kernel methods) can also be applied to the calculation of concentrations (Lynch et al., 2015; page 290).

Radionuclides are, in general, transported in dissolved and solid phases. Exchanges of radionuclides between the liquid and solid phases occur in a continuous (and reversible) form along the simulated time. These processes are easily described in Eulerian models, since only a few additional terms should be added to the differential transport (advection–diffusion) equation (see details for instance in Periáñez, 2005b). However, in a Lagrangian model we are working with individual particles which can be either in dissolved form or in the solid phase. It is necessary to decide, each time step along the simulation, if each particle is changing its state or not. This is done using a stochastic approach. The phase transition probabilities in particle tracking models can be described as Markov processes in systems which jump from one state to another in a continuous time. Therefore, it is relevant to estimate the dependence of the transition probabilities values with the time step used to integrate the model.

The International Atomic Energy Agency (IAEA) has launched several programs with the objectives of, among others, testing and improving numerical models which simulate the transport of radionuclides in the environment, as EMRAS, EMRAS–II, MODARIA and MODARIA–II, which is the latest effort. Interest in the marine environment increased after Fukushima Dai–ichi NPP accident in 2011. The marine working group in MODARIA and MODARIA–II was involved in radionuclide transport modelling for the marine environment; modelling Fukushima releases in the Pacific Ocean was one of the addressed problems (Periáñez et al., 2015, 2019b IAEA, 2019). Lagrangian models were applied to this problem and model–model and model–data comparisons were carried out (see references above). However, it is difficult to evaluate the causes of the differences in results between models in such a complex natural environmental system where we have spatio–temporal changing current fields with the generation of eddies, interactions of radionuclides with sediments and a complex source term (variable direct releases from Fukushima into the ocean and deposition from the atmosphere over a large portion of the ocean). Consequently, very simple radionuclide transport problems were posed with the objective of investigating the dependence of a Lagrangian transport model to grid spacing, number of particles, interpolation schemes and dependence of phase transition probabilities with the time step. This could help to understand the functioning of the most basic aspects of Lagrangian transport models, which in turn can lead to improved models which could be used in the future.

A brief description of Lagrangian techniques is included in sections 2.1 and 2.2. The simple 1D transport problems used for the analysis are presented in section 2.3. The dependence of results with grid spacing and number of particles is analyzed in section 3.1, and the interpolation schemes in section 3.2. The dependence of phase transition probabilities with the time step is studied in section 3.3. Finally, the one–dimensional scavenging problem was considered in section 3.4, which combines one–dimensional transport and phase transitions. This realistic example is used to study the limitation to the time step introduced in Lagrangian models by phase transitions.

2. Methods

2.1. Lagrangian transport models

In Lagrangian models the released activity is represented by a number of particles, each one equivalent to a given amount of activity (Bq) as mentioned above. The path followed by each particle is calculated and radionuclide concentrations are evaluated from the number of particles per volume unit. The equations describing the change in a particle position over each time increment dt are given by the Itô (Protter, 2004) stochastic differential equations:

$$dx = u\,dt + \frac{\partial K_h}{\partial x}dt + \sqrt{2K_h}dW_x, \tag{1}$$

$$dy = v\,dt + \frac{\partial K_h}{\partial y}dt + \sqrt{2K_h}dW_y, \tag{2}$$

$$dz = w\,dt + \frac{\partial K_v}{\partial z}dt + \sqrt{2K_v}dW_z, \tag{3}$$

where u, v and w are velocity components along coordinate axis (x, y, z); and W_x, W_y, W_z are independent components of the stochastic motion, which have zero mean and variance dt ($\overline{dW_x^2} = \overline{dW_y^2} = \overline{dW_z^2} = dt$). For a finite time step Δt they can be simulated as $\Delta W_x = \sqrt{\Delta t}R_x$, $\Delta W_y = \sqrt{\Delta t}R_y$, $\Delta W_z = \sqrt{\Delta t}R_z$, where (R_x, R_y, R_z) are normally distributed random variables having zero mean and standard deviation one. In practice they can be obtained, in FORTRAN for instance, from the `random_number` function. Derivatives of the diffusion coefficients above prevent the artificial accumulation of particles in regions of low diffusivity (Proehl et al., 2005; Lynch et al., 2015). Zero or constant diffusion coefficients are used in the present work, thus these term are not relevant.

As mentioned before, although a grid is not required to evaluate diffusion and advection, it is generally used to calculate the radionuclide concentrations from the position of particles (although there are also meshless methods for the calculation of concentration as already mentioned): grid cells are defined, then the number of particles inside each cell is counted and the resulting concentration C is the total activity within the cell divided by the cell volume:

$$C = \frac{1}{V}\sum_{i=1}^{N} R_i \tag{4}$$

where R_i is the number of Bq equivalent to particle i, N is the number of particles within the considered cell and V is its volume.

While there is no stability criterion equivalent to the Eulerian CFL (Courant–Friedrichs–Levy) condition (Kowalik and Murty, 1993) in the particle–tracking calculations, it is wise to ensure that in a realistic application of a Lagrangian model each particle does not move through a distance that exceeds the grid spacing (used by the hydrodynamic

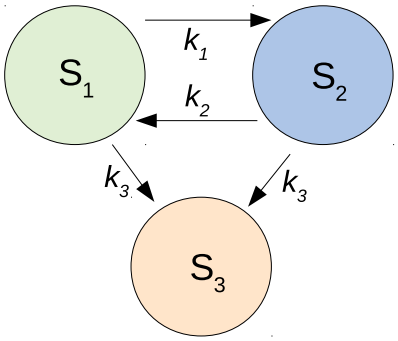

Fig. 1. Graph of phase transitions in a three–state system.

model to generate water currents) during each time–step. Thus, maximum time step is given by:

$$\Delta t < \frac{\Delta x}{u_{max}} \tag{5}$$

where Δx is grid spacing and u_{max} is the maximum water velocity.

The review paper Periáñez et al. (2019a) discusses typical spatial and temporal resolutions of models, which depend on the particular problem to be addressed.

2.2. The master equations to describe phase transitions

Consider a three phase system where exchanges of radionuclides between the dissolved state and the solid matter are described by kinetic coefficients k_1 and k_2, and where radionuclide decay constant is k_3. The activities in dissolved and solid matter phases are A_1 and A_2 (Bq), respectively, whereas A_3 represents lost activity due to the radioactive decay ($A_1 + A_2 + A_3 = \mathbf{const}$). The corresponding equations describing this system are:

$$\frac{\partial A_1}{\partial t} = -k_1 A_1 + k_2 A_2 - k_3 A_1, \tag{6}$$

$$\frac{\partial A_2}{\partial t} = k_1 A_1 - k_2 A_2 - k_3 A_2, \tag{7}$$

$$\frac{\partial A_3}{\partial t} = k_3 A_1 + k_3 A_2, \tag{8}$$

where t is time. The activity in the considered volume can be represented as consisting of N identical particles being in three phases S_1, S_2 and S_3 as shown in Fig. 1. Then the activity is distributed in these possible phases as $p_1 N$, $p_2 N$ and $p_3 N$, where p_1, p_2 and p_3 are the probabilities of radionuclide particles to be in each corresponding phase. Then equations (6)-(8) can be rewritten in form of the differential equations for the probability evolutions which describe the Markov processes in systems which jump from one state to another in continuous time. These equations (master equations) are equivalent to the Kolmogorov forward equations. They are written as:

$$\frac{\partial p_1}{\partial t} = -k_1 p_1 + k_2 p_2 - k_3 p_1, \tag{9}$$

$$\frac{\partial p_2}{\partial t} = k_1 p_1 - k_2 p_2 - k_3 p_2, \tag{10}$$

$$\frac{\partial p_3}{\partial t} = k_3 p_1 + k_3 p_2. \tag{11}$$

The solution of this system of equations with initial conditions $p_1(0)$, $p_2(0)$ and $p_3(0) = 0$ is:

$$p_1(t) = \frac{k_2}{k_1 + k_2} \times \left(\frac{k_1 p_1(0) - k_2 p_2(0)}{k_2} e^{-(k_1+k_2+k_3)t} + (p_1(0) + p_2(0)) e^{-k_3 t} \right) \tag{12}$$

$$p_2(t) = \frac{k_1}{k_1 + k_2} \times \left(\frac{k_2 p_2(0) - k_1 p_1(0)}{k_1} e^{-(k_1+k_2+k_3)t} + (p_1(0) + p_2(0)) e^{-k_3 t} \right) \tag{13}$$

$$p_3(t) = 1 - e^{-k_3 t}. \tag{14}$$

The transition probability p_{ij} defines the probability that a particle in state i is transferred to state j during a time step Δt. These transition probabilities are used in Lagrangian models to decide if the state change occurs or not. Thus, for each particle and time step a independent random number RAN between 0 and 1 is generated. If $RAN \leq p_{ij}$ then the change from i to j occurs. In practice, a label is assigned to each particle, which identifies its state. The label is changed accordingly to its state changes.

The transition probabilities $p_{1,2}$ and $p_{1,3}$ during the time step Δt are obtained from (12)-(14) using the initial conditions $p_1(0) = 1$, $p_2(0) = 0$, $p_3(0) = 0$ and relationship (19), shown below. They are written in non–dimensional form as

$$p_{1,2} = p_2(\Delta t) = \frac{m k_d}{m k_d + 1} \times \left[\exp\left(-\frac{k_3}{k_1} \Delta t^* \right) - \exp\left(-\left(1 + \frac{1}{m k_d} + \frac{k_3}{k_1} \right) \Delta t^* \right) \right], \tag{15}$$

$$p_{1,3} = 1 - \exp\left(-\frac{k_3}{k_1} \Delta t^* \right), \tag{16}$$

where $\Delta t^* = k_1 \Delta t$. Additionally, the transition probabilities $p_{2,1}$ and $p_{2,3}$ during the time step Δt are obtained as

$$p_{2,1} = p_1(\Delta t) = \frac{1}{m k_d + 1} \times \left[\exp\left(-\frac{k_3}{k_1} \Delta t^* \right) - \exp\left(-\left(1 + \frac{1}{m k_d} + \frac{k_3}{k_1} \right) \Delta t^* \right) \right], \tag{17}$$

$$p_{2,3} = 1 - \exp\left(-\frac{k_3}{k_1} \Delta t^* \right). \tag{18}$$

To arrive to this form of the equations, the coefficient k_2 is written as a function of k_1 and the radionuclide distribution coefficient k_d ($m^3 kg^{-1}$). The following relation holds (Periáñez et al., 2018):

$$k_d = \frac{1}{m} \frac{k_1}{k_2}, \tag{19}$$

where m is the concentration of sediment (kg m^{-3}). In practical applications it is more convenient to fix k_2, since Nyffeler et al. (1984) found small differences in this parameter between elements. This coefficient k_2 is usually defined as $k_2 = 1.16 \times 10^{-6}$ s^{-1}, which was obtained from the experiments in Nyffeler et al. (1984). This value has been used in many previous published modelling works [see review in Periáñez et al. (2019a)] and also it was applied to different chemical elements. k_d values can be obtained from the compilation given in IAEA (2004). The sediment concentration m obviously depend on the site where the model is applied. Thus, k_1 is derived from m, k_2 and k_d using equation (19) and then included in the transition probabilities equations above.

Once a particle has decayed (it is in state S_3) it is removed from the computations, thus there are not transition probabilities p_{31} and p_{32}. The coefficient k_3 is the radioactive decay constant of the radionuclide: $k_3 = \lambda$.

2.3. Physical setup of the problems

Two one–dimensional cases are considered, horizontal (longitudinal) transport in a tidal channel and a scavenging process in a water column. They are described in the following two sections.

2.3.1. Transport in a channel

A simple 1D problem was considered, consisting of radionuclide transport along a channel with constant geometry, to evaluate model dependence with grid spacing and interpolation schemes. A tide propagates in the channel and water currents and depths change in time and

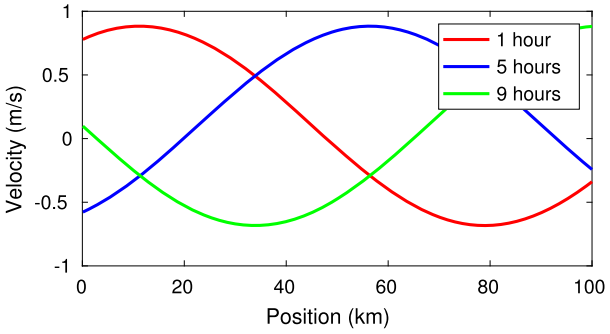

Fig. 2. Water velocities along the tidal channel at three times.

space. Channel width is not relevant since the exercises are 1D, thus results are averaged over the channel width.

The tidal channel is 100 km long. The period of the tide is 12 hours and its amplitude $H_0 = 0,25$ m. The channel depth is constant and equal to $D = 1$ m. From the analytical solution of the 1D wave equation water velocities and surface elevations along the channel can be calculated at any time and position. Equations for wave propagation in a non–rotating system are the following (Pugh, 1987):

$$z(x,t) = H_0 \cos(kx - \omega t) \tag{20}$$

$$u(x,t) = H_0 (g/D)^{1/2} \cos(kx - \omega t) \tag{21}$$

where z is surface elevation, u is water velocity, g is gravity; and angular speed ω and wave number k are related through the wave speed c:

$$c = \frac{\omega}{k} = \sqrt{g\,D} \tag{22}$$

These equations are used to generate data, which are saved in 12 files (one per hour) to be read by the transport codes. The channel is divided into 1000 cells (segments in this case) with $\Delta x = 100$ m. Each file contains the water velocity and elevation in the center of each cell from equations given above. In addition to the tide, a net residual current (net transport) to the right, equal to 0,1 m/s, is included. The 12 files contain velocity and elevation profiles along the channel at $t = 1$ h, $t = 2$ h etc. The sequence is repeated to simulate as many days as required. As an example, three of the velocity profiles along the channel are given in Fig. 2. It may be seen that the tide propagates towards the right side of the channel; this way a consistent pattern in which currents change in time and space is produced. It is considered that the channel is open at both left and right sides, thus if a particle leaves the channel it is simply removed from the computation.

A constant horizontal (longitudinal) diffusion coefficient equal to 1 m^2/s is considered. Instantaneous mixing in the transverse direction is assumed; in addition vertical diffusion is not added. Two problems are treated: a single–particle movement and deposition of radionuclides over a segment of the channel:

1. A single particle is released on the surface (although this is not relevant) at position $x = 10$ km from the left side of the channel at $t = 0$. Its position is calculated during 6 tidal cycles (72 hours). Horizontal diffusion is not considered in this case.
2. An initial deposition of 100 Bq/m^2 occurs on the first 500 m of the channel over a 1 m thick surface layer. The endpoint of the calculation is to provide a profile of radionuclide concentration along the channel length surface after 6 tidal cycles (72 hours).

2.3.2. Modelling the scavenging process

The scavenging process is considered as a realistic example of a one–dimensional transport problem which additionally includes phase transitions. Scavenging of particle–reactive elements is the process by which dissolved radionuclides are removed from a water column by adsorption onto settling particulate matter which eventually deposits on the bed sediment.

The differential equations (i.e., Eulerian equations) describing this process are presented in what follows. They allow to obtain a self–similar solution. The Lagrangian approach solution will then be compared with these self–similar solutions.

An idealized one–dimensional problem consisting of the vertical spreading of a radionuclide due to diffusion and suspended multifraction particulate matter settling in a water column, in which advection by currents is neglected, is considered (Periáñez, 1998; Maderich et al., 2021). The sorption–desorption processes between the dissolved state ($\alpha = 1$) and particulate states $\alpha = 2 \ldots n$, where n is the total number of states, is described by a first order kinetics. The general equation for the concentration (C_d, Bq/m^3) in the dissolved phase ($\alpha = 1$) is (Maderich et al., 2017):

$$\frac{\partial C_d}{\partial t} = \frac{\partial}{\partial x}\left(D\frac{\partial C_d}{\partial x}\right) - \lambda C_d - k_2\left(C_d \sum_{\alpha=2}^{n} S_{p,\alpha} k_{d,\alpha} - C_p\right) \tag{23}$$

where the vertical coordinate x is measured downwards from the surface, D (m^2/s) is the diffusion coefficient, λ the radioactive decay constant, $S_{p,\alpha}$ is the concentration of suspended matter (kg/m^3) in state α and the distribution coefficient $k_{d,\alpha}$ is related to the equilibrium values of dissolved and particulate radionuclide concentrations (equation (19)):

$$S_{p,\alpha} k_{d,\alpha} = \frac{C_{p,\alpha}^{eq}}{C_d^{eq}} \tag{24}$$

and the total radionuclide concentration in the particulate phase C_p is given by:

$$C_p = \sum_{\alpha=2}^{n} C_{p,\alpha} \tag{25}$$

The equation for the radionuclide concentration in the particulate state α, $C_{p,\alpha}$ (Bq/m^3), is:

$$\frac{\partial C_{p,\alpha}}{\partial t} = -\frac{\partial (w_{p,\alpha} C_{p,\alpha})}{\partial x} + \frac{\partial}{\partial x}\left(D\frac{\partial C_{p,\alpha}}{\partial x}\right) - \lambda C_{p,\alpha} + k_2 (C_d S_{p,\alpha} k_{d,\alpha} - C_{p,\alpha}) \tag{26}$$

where $w_{p,\alpha}$ (m/s) is the settling velocity of particles in α state.

These are the general equations describing the scavenging process, which generalize the scavenging model described in Periáñez (1998). A simplified problem was considered in which λ is neglected and only dissolved ($\alpha = 1$) and one particulate state ($\alpha = 2$) are considered. Thus $k_{d,2} = k_d$, $S_{p,2} = S_p$ and $w_{p,2} = w_p$. Diffusion coefficient D is considered constant and an instantaneous activity I_0 (Bq/m^2) is initially deposited in the surface and introduced in the dissolved state. In these conditions, a self–similar solution of the equations gives for the dissolved phase (Maderich et al., 2021):

$$C_d(x,t) = \frac{I_*}{\sqrt{4\pi D_* t}} \exp\left[-\frac{(x - Ut)^2}{4 D_* t}\right] + O(t^{-1}) \tag{27}$$

where:

$$I_* = \frac{I_o k_2}{k_1 + k_2} = \frac{I_0}{1 + S_p k_d}, \tag{28}$$

$$U = \frac{w_p k_1}{k_1 + k_2} = \frac{w_p S_p k_d}{1 + S_p k_d}, \tag{29}$$

$$D_* = D + \frac{w_p^2 k_1 k_2}{(k_1 + k_2)^3} = D + \frac{w_p^2 S_p k_d}{k_2 (1 + S_p k_d)^3}. \tag{30}$$

3. Results

The dependence of model results with the grid spacing using to calculate concentrations and with the number of particles in the simulation

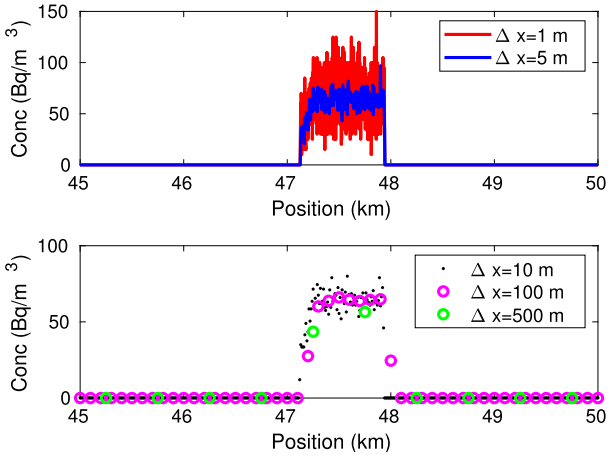

Fig. 3. Radionuclide concentrations along the channel surface calculated for different values of Δx.

is analyzed is section 3.1 and the use of interpolation schemes in section 3.2. The dependence of phase transition probabilities with time step is studied in 3.3 and, finally, the scavenging example is presented in section 3.4. Several institutes have participated in these exercises and repeatability of results was checked.

3.1. Dependence with grid spacing and number of particles

The deposition problem on the tidal channel problem was used for this study. The endpoint of the calculation was to provide a profile of radionuclide concentrations along the channel 72 hours after deposition. Different values of the grid spacing Δx, required to evaluate concentrations from equation (4), were used. Horizontal diffusion coefficient was initially set to zero.

For computational economy, it is natural to use the same grid applied to generate water circulation for evaluating radionuclide concentrations as well, thus this implies that $\Delta x = 100$ m. Other values have been tested and results are presented in Fig. 3, which shows the final radionuclide concentrations along the channel after 72 hours for a number of different Δx choices. The graphic was separated in two panels for better clarity. In the lower panel, where Δx values are larger, results are drawn as a single dot in the middle of each grid cell to reduce a artificial displacement in the patch due to the plotting computer routine.

Mass conservation was checked and the maximum error in results in Fig. 3 was $0,99\%$, which was obtained for the case with $\Delta x = 500$ m. It is most likely due to rounding errors introduced in the calculation of concentrations. In cases with smaller Δx, the error in mass conservation is strictly $0,0\%$.

It can be seen that noise, with overshooting above initial concentrations, is generated for Δx values smaller than 10 m. Non–physical concentrations are generated, although mass is conserved. A large Δx (500 m) produces a significant lowering of peak concentration. Some noise is generated with $\Delta x = 10$ m as well. In this particular exercise reasonable results (low noise and relatively small artificial diffusion) are obtained if $\Delta x = 100$ m.

If the number of particles in the simulation increases (10000 particles were used in calculations shown in Fig. 3) then the statistics, understood as number of particles within each grid cell, improves and noise decreases. However, noise is not totally removed at low Δx values in spite of increasing the number of particles by orders of magnitude, with the increase in computational cost which this implies. Fig. 4 shows results in Fig. 3 for $\Delta x = 1$ m with 10^4 particles (as in Fig. 3) and also with 10^6 particles.

In all cases the concentration is reduced with respect to the initial deposition of 100 Bq/m^2. It is due to the spatio–temporal variations of the tidal currents, since the front edge of the patch will be moving with

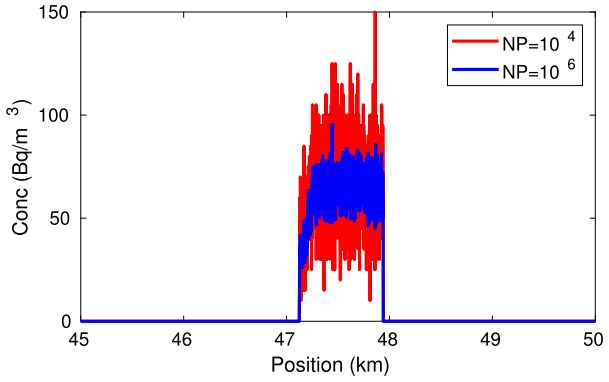

Fig. 4. Radionuclide concentrations along the channel surface calculated for $\Delta x = 1$ m with two different number of particles.

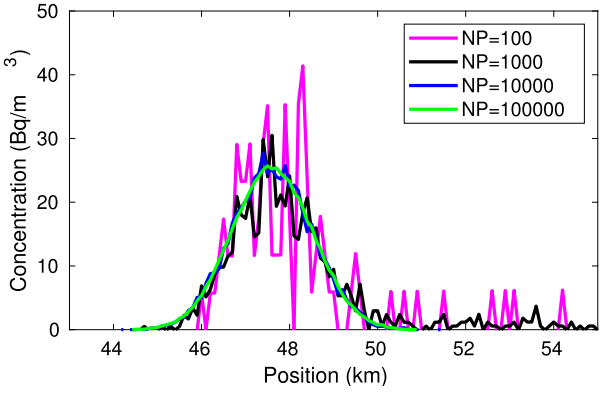

Fig. 5. Radionuclide concentrations along the channel surface calculated for different values of NP. (For interpretation of the colours in the figure(s), the reader is referred to the web version of this article.)

different velocity than the rear and thus a spreading of the radionuclide patch occurs. For instance, if the initial contamination patch is within only one grid cell and after the simulation the same patch (diffusion is not considered) is shared between two cells, the concentrations will necessarily be half than initially.

In this regard, grid cells must be smaller than the deposition area to avoid a artificial reduction of peak concentrations. But if cell size is too small, then the noise problems arise. It seems that, in general, the optimum grid size used to evaluate radionuclide concentrations from the distribution of particles in a Lagrangian model should be tested since these problems may of course be present in realistic scenarios. In these cases, however, they might remain occasionally unnoticed due to the complex water circulation schemes and the generally larger turbulent mixing.

The number of particles used in the simulation, denoted NP, of course affects the quality of results. A value NP = 10000 was used in the simulations in Fig. 3, as mentioned before. The exercise has been repeated (with $\Delta x = 100$ m), now including horizontal diffusion to deal with the full problem, using different NP values. Results are presented in Fig. 5. Of course, the distribution is wider than in Fig. 3 and peak concentrations are lower due to mixing. This problem is simple, and therefore an estimation of the uncertainties in concentrations presented in Fig. 5 can be carried out: since the total distribution width (cells with concentration above zero) is of the order magnitude of 10^2 (10 km), the average number of particles into each cell at the end of the simulation is of the order of NP/10^2. This figure ranges from 1 (NP = 100) to 10^3 (NP = 10^5).

If it is assumed that the number of particles within a grid cell (if the simulation is repeated many times) follows a Gaussian distribution (turbulent mixing is a stochastic process, as it is radioactive decay), then

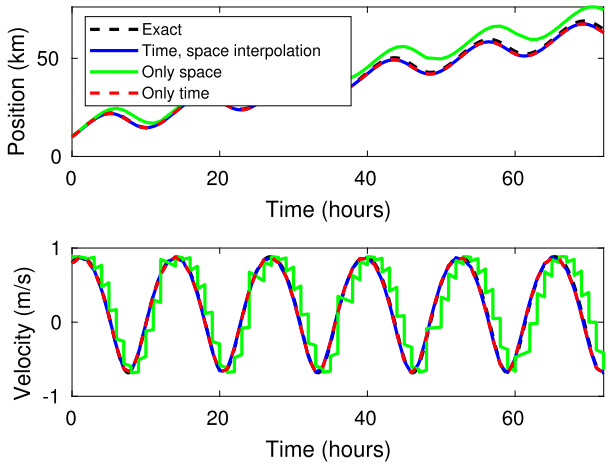

Fig. 6. Temporal evolution of the particle position (top) and velocity (bottom) as calculated with different interpolations. Position is measured from left side of the channel.

an analogy with radioactive counting statistics (García–León, 2022) can be carried out. If a radioactive sample is measured and the number of counts in the detector is N_c, then the probability distribution of the number of counts obtained is well defined with a single parameter, N_c, and the uncertainty is in good approximation $\sigma \sim \sqrt{N_c}$ (García–León, 2022). Therefore, under the considered assumption, the relative error of the radionuclide concentration in a given grid cell i of a model can be estimated as:

$$\sigma_r = \frac{\sqrt{NP_i}}{NP_i} \tag{31}$$

where NP_i is the number of particles within grid cell i. Consequently, the relative errors of concentrations in Fig. 5 are estimated as 100% (NP = 100), 32% (NP = 1000), 10% (NP = 10^4) and for NP = 10^5 it is 3.2%. These estimations agree with the deviations with respect to the green curve in Fig. 5 (which can be considered close to the true solution of the problem; error only 3.2%).

This method of estimating the uncertainty can used to optimize the number of particles in order to have a certain accuracy in Lagrangian simulations. In a preliminary calculation the area covered by the radionuclide patch (after an accident for instance) can be estimated. The average number of particles in each grid cell to have a certain relative error is derived from equation (31) and knowing the number of cells affected by the contamination patch the total number of particles is obtained.

3.2. Interpolation schemes

The single particle release in the tidal channel problem was used to test the effects of using interpolation in time and/or space. Several numerical experiments were carried out, which involved the use of interpolation in both time and space; only interpolation in space and only in time. In addition, the exact solution was calculated from the velocity given by the wave equation solution (equation [(21)]). Only linear interpolation schemes were tested. For real applications the effects of turbulence will mask any small differences in the interpolation schemes, as noted by Elliott and Clarke (1998).

Results of the experiments are presented in Fig. 6. The time evolution of the particle position is shown in the top panel, and the time evolution of water velocity at the particle position in the bottom one.

Using both time and space interpolation mimics the exact solution, but the same situation is obtained if only time interpolation is used. In contrast, a larger error appears if interpolation in time is not used (only spatial interpolation). In this case, the final particle position diverges about 10 km from the exact value. It can be concluded that it is more important to use temporal interpolation than spatial interpolation to have a solution closer to the exact one.

This conclusion is correct for the experiment parameters used in the study because the corresponding wave length of the tide is about 135 km, whereas the initial length of contamination is 0.5 km. In general both temporal and spatial interpolation can affect results. However, in practical situations the size of the radionuclide distribution is much smaller than actual tide wavelengths (of the order of 10^3 km), unless we are interested in transport at full oceanic scales of fallout radionuclides, for instance. But this is not the case in emergency applications, where the interest lies at local to regional scales. Other dynamic features of the ocean with smaller scales are wind waves and capillarity waves (Knauss, 1997; Open University, 2005). Seiches are standing waves which produce a slow oscillation of the water level. They can occur in lakes, as well as in bays, estuaries or harbours which are open to the sea at one side. However, all these wave motions produce horizontal currents which are negligible in comparison with tidal currents. Therefore their effects in radionuclide transport is not significant.

Thus, from a practical point of view, it may be concluded that it is more important to use temporal than spatial interpolation.

3.3. Dependence of phase transition probabilities to the time step using solutions of the master equations

We are going to analyze the dependence of phase transition probabilities with the time step using exact and approximate solutions of the master equations.

The transition probabilities were estimated by Periáñez and Elliott (2002) as:

$$p_{1,2} = 1 - \exp\left(-k_1 \Delta t\right), \qquad p_{2,1} = 1 - \exp\left(-k_2 \Delta t\right), \tag{32}$$

$$p_{1,3} = p_{2,3} = 1 - \exp\left(-k_3 \Delta t\right). \tag{33}$$

Expanding the solution of the equations (9)-(11) in a series of powers of $k_1 \Delta t$ and $k_2 \Delta t$, respectively, and restricting ourselves to first-order terms, we obtain transition probabilities in the form:

$$p_{12}(\Delta t) \approx k_1 \Delta t, \qquad p_{13}(\Delta t) \approx k_3 \Delta t, \tag{34}$$

$$p_{21}(\Delta t) \approx k_2 \Delta t, \qquad p_{23}(\Delta t) \approx k_3 \Delta t \tag{35}$$

The variations of $p_{1,2}$ with non–dimensional time, calculated from the exact formula (15) for three values of mk_d ($mk_d = 0.1; 1; 10$) and for $k_2 = 1.16 \cdot 10^{-5}$ and $k_3 = 1.06 \cdot 10^{-8}$, are compared with equations (32) and (34) in Fig. 7. Note that the $k_3 = \lambda$ value used in the example corresponds to a half–life of 2.07 year, which is the one of ^{134}Cs (taken as an example) and the k_2 is the value obtained by Nyffeler et al. (1984) for Cs, mentioned in section 2.2. Finally a range of typical mk_d product values found in the environment is used (Duursma and Carroll, 1996; IAEA, 2004).

As may be seen in the figure, at small $k_1 \Delta t$ the dependence of $p_{1,2}$ on time step is linear and close for all equations. However, at moderate time step the exact solution depends on mk_d, i.e., for these time steps $p_{1,2}$ can depend both on sediment concentration and the k_d. Notice that the approach (34) can be applied for any number of states, but its use is restricted to small time steps and corresponding small values of the transition probabilities, which guarantees only a single phase change during each time step. The drawback of this approach is that a very small time step is required for fast reactions (Kinzelbach, 1988). The formula (32) works well for large values of mk_d, i.e., high sediment concentration and/or large k_d, but when small values of mk_d are found in the environment the exact solution should be used.

These points should be taken into account to define transition probabilities when a Lagrangian model including exchanges between phases is designed.

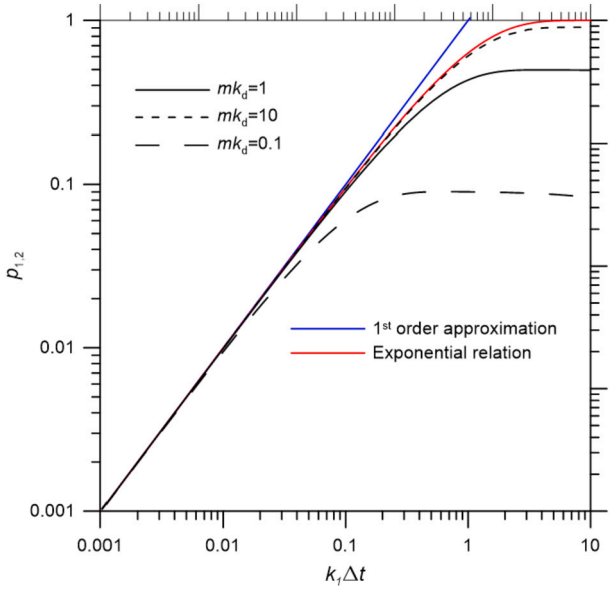

Fig. 7. Dependence of the phase transition probability $p_{1,2}$ on non-dimensional time step $k_1\Delta t$.

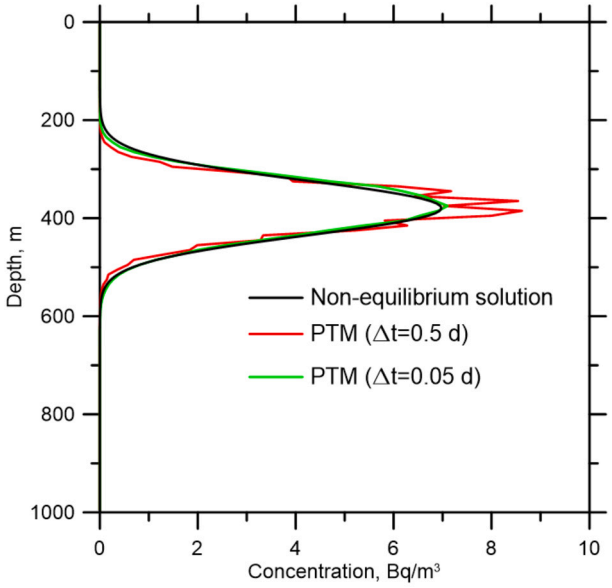

Fig. 8. Solution of the scavenging equation (equation (27)) and particle tracking method (PTM) solution with two values of the time step.

3.4. The scavenging process

A comparison of the self–similar solution (equation (27)) and the particle tracking method (PTM) solution at $t = 10$ year can be seen in Fig. 8. Characteristic parameters of oceanic scales and for ^{240}Pu were used: depth $H = 4000$ m, concentration of particulate matter $S_p = 0.25 \times 10^{-3}$ kg/m^3, settling velocity $w_p = 5 \times 10^{-5}$ m/s, diffusivity $D = 0$, distribution coefficient $k_d = 100$ m^3/kg, desorption coefficient $k_2 = 1.16 \times 10^{-5}$ s^{-1}, and $I_0 = 1$ Bq/m^2. For this isotope $\lambda = 3.4 \times 10^{-12}$ s^{-1}, thus radioactive decay can effectively be neglected. More details on the method, selection of parameters and its application to the scavenging processes are given in Brovchenko and Maderich (2021).

It can be seen in Fig. 8 that phase transitions result in additional dispersion. Also, it may be seen that the simulation with $\Delta t = 0.05$ day fits the analytical solution better than with $\Delta t = 0.5$ day.

The following stability condition is introduced in an Eulerian model by the terms describing water/sediment interactions (Periáñez, 1995b):

$$\Delta t << \frac{1}{k_{max}} \tag{36}$$

where k_{max} is the maximum kinetic rate involved in the problem. Physically it means that the amount of radionuclides transferred from one phase to another must be smaller than the content in the origin phase. Results in Fig. 8 confirm that this limitation holds in the particle tracking method: at $\Delta t = 0.5$ day $k_2\Delta t \approx 0.48$, while if $\Delta t = 0.05$ day then $k_2\Delta t \approx 0.048$. This limitation to the time step must be taken into account in any problem in which phase transitions are present, not only in scavenging processes.

4. Conclusions

Simple one–dimensional transport problems were defined to study the Lagrangian model output dependence with regards to grid spacing, number of particles in the simulation and interpolation schemes.

In general, the optimum grid size used to evaluate radionuclide concentrations from the distribution of particles in a Lagrangian model should be tested. If it is too large a significant artificial diffusion is produced. In contrast, with too small values results might suffer from artificial noise and overshooting of concentrations above the initial peak magnitude. A method to optimize the number of particles required to achieve a given accuracy level in a simulation has been proposed.

With respect to the interpolation schemes required to evaluate the water current at the particle position and at a given time, it may be concluded that it is more important to use temporal interpolation than spatial interpolation to have a solution closer to the exact one. This conclusion seems to be generally correct unless we are interested in transport at full oceanic scales, which is not the case in emergency applications of Lagrangian models.

It was found that an approximate expression for the transition probabilities between phases cannot always be applied, but it depends on the sediment concentration, radionuclide distribution coefficient and time step. In particular, the exact solution should be used for small values of mk_d.

Finally, a one–dimensional scavenging process, as a realistic example combining transport and phase transitions, was considered in a Lagrangian frame. It was found that a limitation to the time step holds, which is linked to the kinetic rates, as it was found to occur in Eulerian models.

Declaration of competing interest

The authors declare that they have no known competing financial interests or personal relationships that could have appeared to influence the work reported in this paper.

Data availability

Data will be made available on request.

Acknowledgement

This work was carried out in the frame of the IAEA MODARIA-II program. It was partially supported by the National Research Foundation of Korea (NRF), by the Korean Government (MSIT) (MSIT:NRF-2017M2A8A4015253, NRF-2015M2A2B2034282) and the National Research Foundation of Ukraine project no. 2020.02/0048. Dr. K.T. Jung and K.O. Kim were supported by KIOST major project (PE99812).

References

Brovchenko, I., Maderich, V., 2021. Modelling radionuclide scavenging in the ocean by particle tracking in multicomponent medium with first-order reaction kinetics. In: Palagin, A., Anisimov, A., Morozov, A., Shkarlet, S. (Eds.), Mathematical Modeling

and Simulation of Systems (MODS'2020). MODS 2020. In: Advances in Intelligent Systems and Computing, vol. 1265. Springer, Cham, pp. 36–46.
Duursma, E.K., Carroll, J., 1996. Environmental Compartments. Springer–Verlag, Berlin.
Elliott, A.J., Clarke, S., 1998. Shallow water tides in the firth of forth. Hydrographic J. 87, 19–24.
García–León, M., 2022. Detecting Environmental Radioactivity. Springer, Switzerland.
Harms, I., Karcher, M.J., Dethleff, D., 2000. Modelling Siberian river runoff - implications for contaminant transport in the Arctic Ocean. J. Mar. Syst. 27, 95–115.
IAEA, 2004. Sediment Distribution Coefficients and Concentration Factors for Biota in the Marine Environment. Technical Reports Series 422, Vienna.
IAEA, 2019. Modelling of Marine Dispersion and Transfer of Radionuclides Accidentally Released from Land Based Facilities, IAEA-TECDOC-1876, Vienna.
Kawamura, H., Kobayashi, T., Furuno, A., In, T., Ishikawa, Y., Nakayama, T., Shima, S., Awaji, T., 2011. Preliminary numerical experiments on oceanic dispersion of ^{131}I and ^{137}Cs discharged into the ocean because of the Fukushima Daiichi nuclear power plant disaster. J. Nucl. Sci. Technol. 48, 1349–1356.
Kinzelbach, W., 1988. The random walk method in pollutant transport simulation. In: Custodio, E., et al. (Eds.), Groundwater Flow and Quality Modeling. D. Reidel, Dordrecht, pp. 227–245.
Knauss, J.A., 1997. Introduction to Physical Oceanography. Prentice–Hall, New Jersey.
Kobayashi, T., Otosaka, S., Togawa, O., Hayashi, K., 2007. Development of a non-conservative radionuclides dispersion model in the ocean and its application to surface cesium-137 dispersion in the Irish Sea. J. Nucl. Sci. Technol. 44 (2), 238–247.
Kowalik, Z., Murty, T.S., 1993. Numerical Modelling of Ocean Dynamics. World Scientific, Singapore.
Lynch, D.R., Greenberg, D.A., Bilgili, A., Mcgillicuddy, D.J., Manning, J.P., Aretxabaleta, A.L., 2015. Particles in the Coastal Ocean. Theory and Applications. Cambridge University Press, NY.
Maderich, V., Jung, K.T., Brovchenko, I., Kim, K.O., 2017. Migration of radioactivity in multifraction sediments. Environ. Fluid Mech. 17 (6), 1207–1231. https://doi.org/10.1007/s10652-017-9545-9.
Maderich, V., Kim, K.O., Brovchenko, I., Kivva, S., Kim, H., 2021. Scavenging processes in multicomponent medium with first–order reaction kinetics: Lagrangian and Eulerian modeling. Environ. Fluid Mech. 21, 817–842. https://doi.org/10.1007/s10652-021-09799-1.
Min, B.I., Periáñez, R., Kim, I.G., Suh, K.S., 2013. Marine dispersion assessment of ^{137}Cs released from the Fukushima nuclear accident. Mar. Pollut. Bull. 72, 22–33.
Nakano, H., Motoi, T., Hirose, K., Aoyama, M., 2010. Analysis of ^{137}Cs concentration in the Pacific using a Lagrangian approach. J. Geophys. Res. 115, C06015.
Nyffeler, U.P., Li, Y.H., Santschi, P.H., 1984. A kinetic approach to describe trace element distribution between particles and solution in natural aquatic systems. Geochim. Cosmochim. Acta 48, 1513–1522.
Open University, 2005. Waves, Tides and Shallow–Water Processes. Butterworth–Heineman, UK.
Periáñez, R., 1998. Modelling the distribution of radionuclides in deep ocean water columns. Application to ^{3}H, ^{137}Cs and ^{239,240}Pu. J. Environ. Radioact. 38, 173–194.
Periáñez, R., 2005a. GISPART: a numerical model to simulate the dispersion of contaminants in the Strait of Gibraltar. Environ. Model. Softw. 20, 797–802.
Periáñez, R., 2005b. Modelling the Dispersion of Radionuclides in the Marine Environment: an Introduction. Springer-Verlag, Heidelberg.
Periáñez, R., Elliott, A.J., 2002. A particle tracking method for simulating the dispersion of non conservative radionuclides in coastal waters. J. Environ. Radioact. 58, 13–33.
Periáñez, R., Bezhenar, R., Min, Byung-Il, Duffa, C., Jung, K., Kobayashi, T., Suh, Kyung-Suk, Lamego, F., Maderich, V., Nies, H., Osvath, I., Psaltaki, M., 2015. A new comparison of marine dispersion model performances for Fukushima releases in the frame of IAEA MODARIA program. J. Environ. Radioact. 150, 247–269.
Periáñez, R., Suh, Kyung-Suk, Min, Byung-Il, 2016. The behaviour of ^{137}Cs in the North Atlantic Ocean assessed from numerical modelling: releases from nuclear fuel reprocessing factories, redissolution from contaminated sediments and leakage from dumped nuclear wastes. Mar. Pollut. Bull. 113, 343–361.
Periáñez, R., Brovchenko, I., Jung, K.T., Kim, K.O., Maderich, V., 2018. The marine k_d and water/sediment interaction process. J. Environ. Radioact. 192, 635–647.
Periáñez, R., Bezhenar, R., Brovchenko, I., Duffa, C., Iosjpe, M., Jung, K.T., Kim, K.O., Kobayashi, T., Liptak, L., Little, A., Maderich, V., McGinnity, P., Min, B.I., Nies, H., Osvath, I., Suh, K.S., de With, G., 2019a. Marine radionuclide transport modelling: recent developments, problems and challenges. Environ. Model. Softw. 122, 104523.
Periáñez, R., Bezhenar, R., Brovchenko, I., Jung, K.T., Kamidara, Y., Kim, K.O., Kobayashi, T., Liptak, L., Maderich, V., Min, B.I., Suh, K.S., 2019b. Fukushima releases dispersion modelling over the Pacific Ocean. Comparisons of models with water, sediment and biota data. J. Environ. Radioact. 198, 50–63.
Proehl, J.A., Lynch, D.R., McGuillicuddy, D.J., Ledwell, J.R., 2005. Modeling turbulent dispersion on the North Flank of Georges Bank using Lagrangian particle methods. Cont. Shelf Res. 25, 875–900.
Protter, P.E., 2004. Stochastic Integration and Differential Equations, 2nd ed. Springer. ISBN 3-540-00313-4.
Pugh, D.T., 1987. Tides, Surges and Mean Sea–Level. Wiley, Chichester, UK.
Schonfeld, W., 1995. Numerical simulation of the dispersion of artificial radionuclides in the English Channel and the North Sea. J. Mar. Syst. 6, 529–544.
Suh, K.S., Park, K., Min, B.I., Kim, S., Kim, J., 2021. Development of a web-based radiological emergency preparedness system for nuclear accidents. Ann. Nucl. Energy 156, 108203.